horticulturae

MDPI

Article

Genome-Wide Analysis of the BBX Gene Family and Their Drought Stress Responses in the Gymnosperm *Torreya grandis*

Weijie Chen [1,2,*,†], Xuanzi Zhang [1,2,†], Xiao Liu [1,2], Fangyan Dai [1,2], Chengjun Zhang [1,2] and Jiasheng Wu [1,2,*]

[1] State Key Laboratory for Development and Utilization of Forest Food Resources, Zhejiang A&F University, Hangzhou 311300, China; zhangxz_zafu@163.com (X.Z.); liuxiao_linder@163.com (X.L.); daifyf@126.com (F.D.); cwj86948968@163.com (C.Z.)

[2] Zhejiang Key Laboratory of Non-Wood Forest Products Quality Regulation and Processing Utilization, Zhejiang A&F University, Hangzhou 311300, China

* Correspondence: weijiechen@zafu.edu.cn (W.C.); wjs@zafu.edu.cn (J.W.)

† These authors contributed equally to this work.

Highlights

What are the main findings?

- Genome-wide identification of 13 *TgBBXs* was completed in *T. grandis*.
- Drought induces tissue-specific differential expression of *TgBBXs* in roots and leaves.

What are the implications of the main findings?

- Three hub *TgBBXs* linked to photosynthesis and drought response were screened by WGCNA.
- This work provides candidate genes for further functional research on BBX transcription factors in gymnosperms.

Abstract

B-BOX (BBX) transcription factors regulate plant growth and drought tolerance, whereas comprehensive characterization of BBX gene families in gymnosperms remains scarce. We identified 13 *TgBBXs* in *Torreya grandis* at the genome-wide level, and phylogenetic analysis grouped them into five subgroups consistent with the conserved classification of plant BBX members. Promoter analysis revealed abundant light hormone and stress related *cis*-elements, and the *TgBBXs* displayed distinct expression patterns across various tissues and reproductive developmental stages. PEG-triggered drought decreased leaf chlorophyll, accompanied by increased root H_2O_2, APX and POD levels. Transcriptome data showed obvious tissue-specific expression and organ-dependent drought responses; most of *TgBBX5*–*TgBBX12* were continuously upregulated in leaves under PEG treatment, whereas several members declined in roots. WGCNA further indicated that the MEturquoise module, which contained most *TgBBXs*, was closely associated with chlorophyll accumulation and antioxidant responses. Among these genes, *TgBBX2*, *TgBBX7*, and *TgBBX13* with module membership over 0.9 are putative hub genes, and their associated genes enrich in photosynthesis and antioxidant pathways. This study systematically characterized the BBX family in *T. grandis* for the first time and identified key drought-responsive genes, providing valuable resources for drought-tolerant molecular breeding of this economically important gymnosperm.

Keywords: *Torreya grandis*; BBX; drought stress

Check for updates

Academic Editor: Gunārs Lācis

Received: 30 June 2026
Revised: 24 July 2026
Accepted: 27 July 2026
Published: 28 July 2026

Copyright: © 2026 by the authors. Licensee MDPI, Basel, Switzerland. This article is an open access article distributed under the terms and conditions of the Creative Commons Attribution (CC BY) license.

1. Introduction

The B-box proteins (BBXs) belong to a family of zinc-finger transcription factors widely distributed in eukaryotes, including animals, plants, and some fungi, with the core feature of containing conserved B-box domains [1–3]. Across plant lineages from basal bryophytes to advanced angiosperms, the BBX family dominates regulatory cascades for growth and diverse stress responses [4]. Most existing studies on the identification and systematic profiling of BBX gene families have centered on angiosperm species. For example, a total of 32 BBX members have been found in Arabidopsis, which are grouped into five phylogenetic clades based on B-box domain counts and the occurrence of CCT domains [5]. Similar analyses across angiosperms show variable BBX counts, including 59 BBX members that have been characterized in *Glycine max* [6], 24 in *Vaccinium darrowii* [7], 30 in *Oryza sativa*, and 36 in *Zea mays* [8,9]. In contrast, far fewer BBX genes have been identified in green algae, a representative group of lower plants, with one member in *Chlamydomonas reinhardtii*, three in *Ostreococcus lucimarinus*, and four in *Ostreococcus tauri* [4]. However, to date, systematic investigations into BBX proteins in gymnosperms and ferns are still relatively scarce.

Currently, functional studies on BBXs have mainly focused on core physiological processes, including photomorphogenesis and light signal transduction, flowering time regulation, organ development and morphogenesis, as well as fruit development and ripening [10]. Notably, CO/AtBBX1 is the first BBX gene isolated in Arabidopsis. In addition, its protein contains a B-box zinc-finger motif and a C-terminal CCT domain. More importantly, it plays a core role in regulating photoperiodic flowering [11]. Further research has demonstrated that the CO-FT module integrates endogenous and environmental signals to fine-tune flowering time. It interacts with key circadian clock factors such as CCA1, LHY and TOC1, as well as the signaling pathways of gibberellin, abscisic acid and auxin [12,13]. Notably, in poplars, this conserved module also exerts a regulatory role in seasonal growth cessation and bud set beyond flowering time, reflecting its functional expansion in woody species [14]. Additional studies show that AtBBX24 interacts with AtHY5 to modulate seedling photomorphogenesis [15], while SlBBX20 promotes anthocyanin biosynthesis by directly binding the promoter of the anthocyanin biosynthetic gene *SlDFR* [16]. These examples indicate that BBX proteins play indispensable roles in multiple plant developmental stages including organogenesis, growth rhythm and reproductive development.

Beyond developmental regulation, the BBX family exerts diverse functions in abiotic stress responses and has been reported to participate in adaptation to multiple stresses including salt, cold and oxidative stress [1]. Notably, as a major environmental constraint limiting plant growth, drought stress elicits distinct functional diversity among different BBXs across various plant species, with its regulatory mechanisms having been systematically investigated in several plants. In *Solanum pennellii*, SpBBX18 interacts with *SpAPX1* and binds to its promoter to mediate drought resistance [17]. In contrast, in *Ipomoea batatas*, IbBBX28 interacts with IbHOX11 and IbZMAT2 and negatively regulates drought tolerance by reducing protective enzyme activities and increasing MDA content [18]. However, functional studies on the BBX family have predominantly focused on angiosperms, leaving their roles in gymnosperms largely unexplored, despite the fact that these evolutionarily ancient plants may possess superior stress resilience.

Torreya grandis is an ancient, long-lived gymnosperm belonging to the Taxaceae family [19]. It is widely cultivated in subtropical China for its nuts, which are valued for their delicious flavor and rich nutritional content. As an economically important species, *T. grandis* exhibits strong drought resistance, a trait derived from its ancient evolutionary origin and long lifespan; this stress resilience is vital to sustaining stable fruit yield and quality in water-limited environments [20–22]. Despite the established pivotal role of BBX

proteins in regulating plant stress responses, their functional characterization in *T. grandis* remains largely unexplored.

To address this gap, a genome-wide survey identified 13 *TgBBXs* in *T. grandis.* This work represents the first comprehensive characterization of the family, covering gene structures, *cis*-acting element distributions, and phylogenetic relationships. Their expression profiles across different tissues were further analyzed, with particular attention to transcriptional dynamics during staminate and ovulate strobilus development. Furthermore, seedlings were subjected to PEG-simulated drought stress, and combined transcriptomic and physiological datasets were employed to dissect the regulatory network of *TgBBX* under drought stress. Collectively, these findings provide valuable gene resources and theoretical references for breeding drought-resistant *T. grandis* rootstocks to stabilize yields in arid planting regions.

2. Materials and Methods

2.1. Plant Materials and Drought Stress Treatment

Six-month-old *T. grandis* seedlings derived from wild germplasm were potted and grown in a controlled chamber. Prior to the simulation drought treatment, the seedlings were transferred to hydroponic culture with one-quarter-strength Hoagland's solution for two weeks of acclimatization. Seedlings with uniform and vigorous growth were selected for subsequent experiments. The culture conditions were set to 14 h light (24 °C, 75% relative humidity) and 10 h dark (22 °C, 75% relative humidity). To simulate drought stress, seedlings were exposed to 1/4-strength Hoagland's solution with 30% *w*/*v* PEG 6000 for 2, 8, and 24 h; controls received 1/4-strength Hoagland's solution only. Three independent biological replicates were established for each treatment group.

2.2. Identification of BBX Family in Plants

Protein sequences of *T. grandis* and other gymnosperms were obtained from the Fishshare and NCBI databases [22]. Hidden Markov model (HMM) searches using the Pfam PF00643 profile were then performed against the proteomes to identify putative B-box transcription factors and build a candidate list. Conserved domain analysis with NCBI-CDD was finally applied to verify the presence of B-box domains [23], yielding the final set of BBX members in *T. grandis* and related gymnosperms.

2.3. Phylogenetic Investigation of the BBX Family

Full-length BBX protein sequences from *T. grandis* and other gymnosperms, together with 32 BBX sequences of *Arabidopsis thaliana* retrieved from TAIR, were aligned with MAFFT [24]. A maximum-likelihood (ML) tree was then built in IQ-TREE using all 116 sequences with default settings and 1000 bootstrap replicates [25]. The final tree was visualized and refined with the Evolview v2 online platform [26].

2.4. Promoter Bioinformatics Analysis of BBX Family

For each TgBBX, 2000 bp sequences upstream of the coding region were extracted from the genome using the GFF file. These sequences were then scanned for putative *cis*-acting regulatory elements with PlantCARE [27]. The distribution of identified elements was visualized using TBtools II [28].

2.5. RNA Sequencing and Transcriptome Analysis

Total RNA was extracted from liquid-nitrogen-ground samples using a TIANGEN RNAprep Pure Plant Kit (DP441, Tiangen Biotech (Beijing) Co., Ltd., Beijing, China). Purified mRNA was used for the cDNA library. Twenty-four independent libraries were built

with three biological replicates for each treatment and sequenced on the Illumina NovaSeq platform at Novogene. After filtering, around 6 Gb of clean data per library was aligned to the reference genome [22] with HISAT2 (v2.2.1) using default parameters. Gene expression levels were quantified as FPKM [29]. Transcriptomic analyses, including PCA, hierarchical clustering heatmaps, and KEGG enrichment, were performed on the OmicShare platform (https://www.omicshare.com/). WGCNA was conducted based on gene FPKM values and corresponding sample trait data. Gene normalization and low-abundance gene filtering were completed following the default built-in procedures of the R WGCNA package. The fixed parameters for network construction were power = 16, min modulesize = 20, network type = signed, deep split = 1, and merge cut height = 0.2. We calculated the topological overlap matrix and performed hierarchical clustering. Modules with pairwise distances below 0.2 were merged. Pearson correlation analysis was applied to assess associations between modules and physiological traits. Genes with high module membership (MM) values were defined as hub genes for screening drought-responsive genes. The tissue- and reproductive stage-specific expression profiles of the *TgBBXs* presented were plotted using FPKM values obtained from transcriptome analysis. All raw transcriptome sequencing data were retrieved from a published work by Lou et al. [22], and these datasets were deposited in the GenBank database under the BioProject accession number PRJNA938254.

2.6. Determination of Chlorophyll Content

The chlorophyll content in fresh leaves of *T. grandis* was determined using the Chlorophyll Assay Kit (BC0995, Solarbio, Beijing, China). After midribs were removed, about 0.1 g of leaf tissue was ground in 1.5 mL extraction buffer in the dark, incubated at room temperature for 30 min, then centrifuged at 4000 rpm for 5 min. The supernatant was collected, and absorbance at 645 nm and 663 nm was measured with a microplate reader. The chlorophyll concentrations were calculated on a fresh weight (FW) basis following the manufacturer's standard formulas:

$$\text{Chlorophyll a (mg/g FW)} = 0.01 \times (21.2 \times A663 - 4.48 \times A645) \times F \div W$$

$$\text{Chlorophyll b (mg/g FW)} = 0.01 \times (38.2 \times A645 - 7.8 \times A663) \times F \div W$$

$$\text{Total chlorophyll (mg/g FW)} = 0.01 \times (33.7 \times A645 + 13.4 \times A663) \times F \div W$$

where F represents the dilution factor and W stands for the fresh weight of leaf samples (g).

2.7. Determination of H_2O_2 Content

The hydrogen peroxide content in *T. grandis* root tips was measured using the H_2O_2 Assay Kit (BC3595, Solarbio, Beijing, China). Approximately 0.1 g of root tip tissue was homogenized in 1 mL pre-cooled acetone (Reagent I) on ice. The homogenate was centrifuged at 8000× *g* for 10 min at 4 °C, and the supernatant was collected. Absorbance at 415 nm was measured with a microplate reader. All H_2O_2 concentrations were calculated on a fresh weight (FW) basis following the manufacturer's standard formula for 96-well plate measurement:

$$H_2O_2 \text{ content (μmol/g FW)} = 32.26 \times (\Delta A + 0.08) \div W$$

where ΔA indicates the absorbance difference and W is the fresh weight of root samples (g).

2.8. Enzyme Activity Assay

Ascorbate peroxidase (APX) activity in *T. grandis* root tips was assayed using the APX Assay Kit (BC0225, Solarbio, Beijing, China). Approximately 0.1 g of root tip tissue was

homogenized in 1 mL pre-chilled extraction buffer on ice. The homogenate was centrifuged at 13,000× *g* for 20 min at 4 °C, and the supernatant was collected. Absorbance at 290 nm was recorded at 10 s and 130 s using a Spark multimode microplate reader (Tecan Group Ltd., Männedorf, Switzerland; manufactured by Tecan Austria GmbH, Grödig, Austria). APX activity was quantified on a fresh weight (FW) basis following the manufacturer's protocol with the simplified formula:

$$\text{APX activity (μmol/g FW)} = 0.0019 \times (\Delta A_sample - \Delta A_blank) \div W$$

Peroxidase (POD) activity was measured using the POD Assay Kit (BC0095, Solarbio, Beijing, China). About 0.1 g of root tip tissue was homogenized in 1 mL pre-cooled extraction buffer on ice. After centrifugation at 8000× *g* for 10 min at 4 °C, the supernatant was used for the assay. Absorbance at 470 nm was read at 30 s and 90 s with a microplate reader. POD activity was also calculated on a fresh weight (FW) basis according to the kit instructions, with the simplified formula:

$$\text{POD activity (U/g FW)} = 9800 \times \Delta A \div W \times F$$

2.9. Statistical Analysis

All experiments were set up with three independent biological replicates (n = 3). Quantitative physiological data are presented as the mean ± standard deviation (SD). One-way analysis of variance (one-way ANOVA) followed by post hoc multiple comparison tests was used to detect statistical differences among four treatment groups: CK, 2 h PEG treatment, 8 h PEG treatment and 24 h PEG treatment. Statistical analyses were conducted using GraphPad Prism 10. Statistical significance was set at $p < 0.05$, and different lowercase letters in figures represent significantly different values between groups.

3. Results

3.1. Identification and Characterization of the BBX Family in T. grandis

First, a genome-wide Hmmer search based on the B-box zinc-finger domain (PF00643) with a threshold of E-value < 1×10^{-5} identified 17 potential BBX members in *T. grandis.* Domain integrity verification was then conducted to confirm their composition and features, and 13 BBX members were finally retained after screening. Application of an identical pipeline to *G. biloba*, *P. tabuliformis*, *W. mirabilis*, *C. panzhihuaensis*, and *G. montanum* identified 14, 23, 13, 11, and 10 BBX members, respectively (Table S1). Among these six gymnosperms, most species possessed 10–14 BBX genes, including 13 in *T. grandis*, while *P. tabuliformis* contained 23 BBX members as an outlier.

To gain insights into the molecular basis underlying BBX protein function in *T. grandis*, detailed analysis was conducted on the amino acid composition and nucleotide sequence variation of the 13 confirmed *TgBBXs* (Figure 1). Conserved motifs of all TgBBX proteins were predicted using MEME, and the motif distribution pattern is displayed in Figure 1A. Conserved domain analysis revealed that these TgBBX proteins could be categorized into four groups based on the number of Bbox1 and CCT domains (Figure 1B). Specifically, TgBBX1–TgBBX5 harbored two Bbox1 domains; TgBBX6–TgBBX9 contained two Bbox1 domains plus an additional CCT domain; TgBBX11–TgBBX13 possessed one Bbox1 domain and one CCT domain; and TgBBX10 carried a single Bbox1 domain only (Figure 1B). The coding sequences of the *13 TgBBXs* ranged from 510 bp to 1653 bp, with 0–4 introns and 1–5 exons, showing obvious structural diversity (Figure 1C).

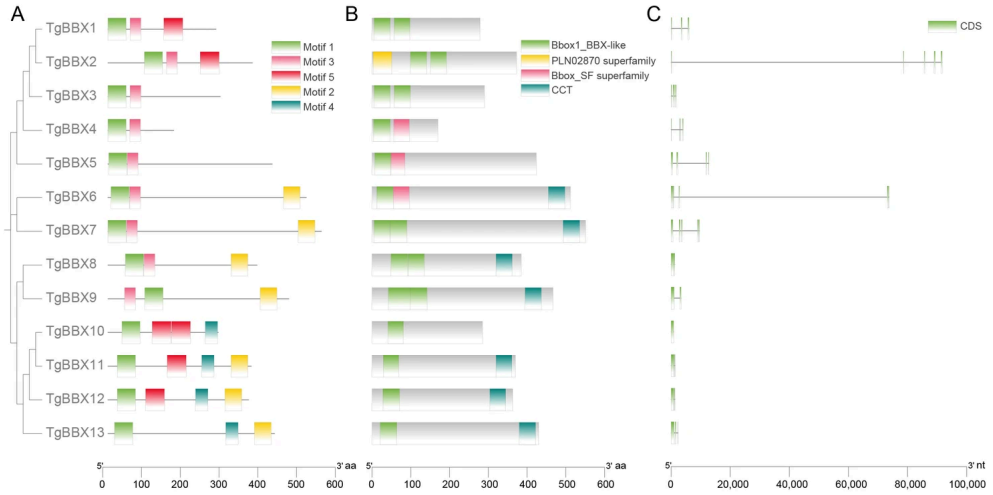


Figure 1. Conserved motif, conserved domain and gene structure distribution of *TgBBXs*. (**A**) Conserved motifs in TgBBX proteins were predicted using MEME. (**B**) Conserved domain distribution of TgBBX identified via NCBI-CDD. (**C**) Exon–intron organization of *TgBBX* coding sequences.

3.2. Phylogenetic Analysis of BBX Proteins in Gymnosperms and A. thaliana

Following the characterization of basic structural features of TgBBX proteins, their phylogenetic relationships with BBXs from major gymnosperm species and *A. thaliana* were further analyzed. For this analysis, a maximum-likelihood (ML) phylogenetic tree was constructed using IQ-TREE based on 116 BBX amino acid sequences from *T. grandis*, *G. biloba*, *P. tabuliformis*, *W. mirabilis*, *C. panzhihuaensis*, *G. montanum*, and *A. thaliana*. As shown in Figure 2, the 116 BBX proteins were classified into five clusters. Furthermore, *A. thaliana* possessed 32 BBX members, which were far more than those identified in each gymnosperm species (Table S1), and these sequences were distributed across all five clusters. Meanwhile, all TgBBXs fell into distinct clades apart from clade 3, which was predominantly occupied by gymnosperm BBXs, with *P. tabuliformis* contributing eight proteins to this group. Similarly, other gymnosperm species such as *G. biloba* and *C. panzhihuaensis* also exhibited distinct distribution patterns and member numbers across different clusters. These results indicate that the BBX exhibits high diversity and abundance in gymnosperms.

3.3. Analysis of Cis-Regulatory Elements in TgBBX Promoters

To explore the potential transcriptional regulation of *TgBBXs*, the 2000 bp sequences upstream of the translation start site of each *TgBBX* were extracted from the *T. grandis* genome. *Cis*-acting elements were predicted using the PlantCARE database and visualized with TBtools. The element distribution diagram in Figure 3A showed that the promoter regions of all *TgBBXs* contained abundant regulatory elements, which were non-uniformly distributed across the promoter region, with most concentrated in the 400–2000 bp range upstream of the translation start site. These elements covered multiple functional categories, including light responsiveness, phytohormone response, stress response, and tissue development regulation. The element abundance heatmap further quantified the enrichment characteristics of *cis*-elements in each *TgBBX* (Figure 3B). Light-responsive elements accounted for more than half of all *cis*-elements and represented the most abundant type in this gene family. Notably, *TgBBX1*, *TgBBX4*, *TgBBX9* and *TgBBX13* each contained more than 15 light-responsive elements. Meanwhile, hormone-responsive elements and environmental response elements were widely distributed across all *TgBBX* promoters. Obvious differences in element abundance were detected among different *TgBBXs*.

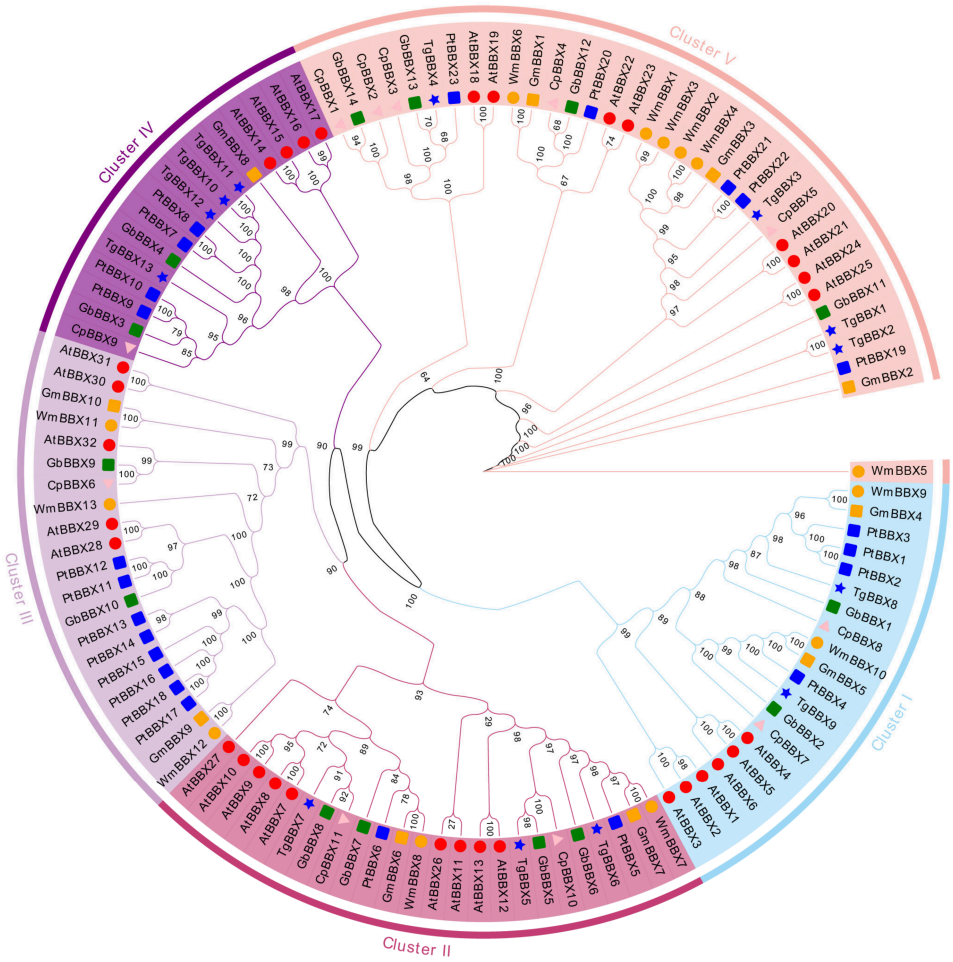


Figure 2. Phylogenetic relationships of BBX proteins from major gymnosperms and *A. thaliana*. The maximum-likelihood phylogenetic tree was constructed based on BBX sequences from the six gymnosperm species *T. grandis*, *G. biloba*, *C. panzhihuaensis*, *G. montanum*, *W. mirabilis* and *P. tabuliformis*, as well as the angiosperm *A. thaliana*. Distinct shapes and colors were applied to label sequences from different species.

3.4. Expression Profiling of the BBX Family in T. grandis

To investigate the potential biological functions of *TgBBXs* in *T. grandis*, expression profiles were systematically characterized across a wide range of tissues and reproductive developmental stages. As illustrated in Figure 4, the 13 *TgBBXs* exhibited highly distinct tissue-specific and stage-specific expression patterns. Within six representative vegetative and reproductive organs, the majority of *TgBBXs* displayed obvious tissue-specific expression preferences. Specifically, *TgBBX1*, *TgBBX2*, *TgBBX4*, and *TgBBX8–TgBBX13* exhibited predominant expression in leaves, with moderate expression detected in stems. Meanwhile, *TgBBX5* and *TgBBX6* displayed dominant expression in arils. In addition, *TgBBX3* was predominantly expressed in roots, and *TgBBX7* showed the highest transcript abundance in seeds (Figure 4A). Further analysis of their expression dynamics across the developmental processes of staminate and ovulate strobili revealed that most *TgBBXs* were highly expressed during the early developmental stages (S1–S5) of staminate strobili (Figure 4B), while they showed high expression levels at the late stages (S4–S5) of ovulate strobili (Figure 4C). These results indicate distinct regulatory roles of *TgBBXs* in the development of different sexual reproductive organs.

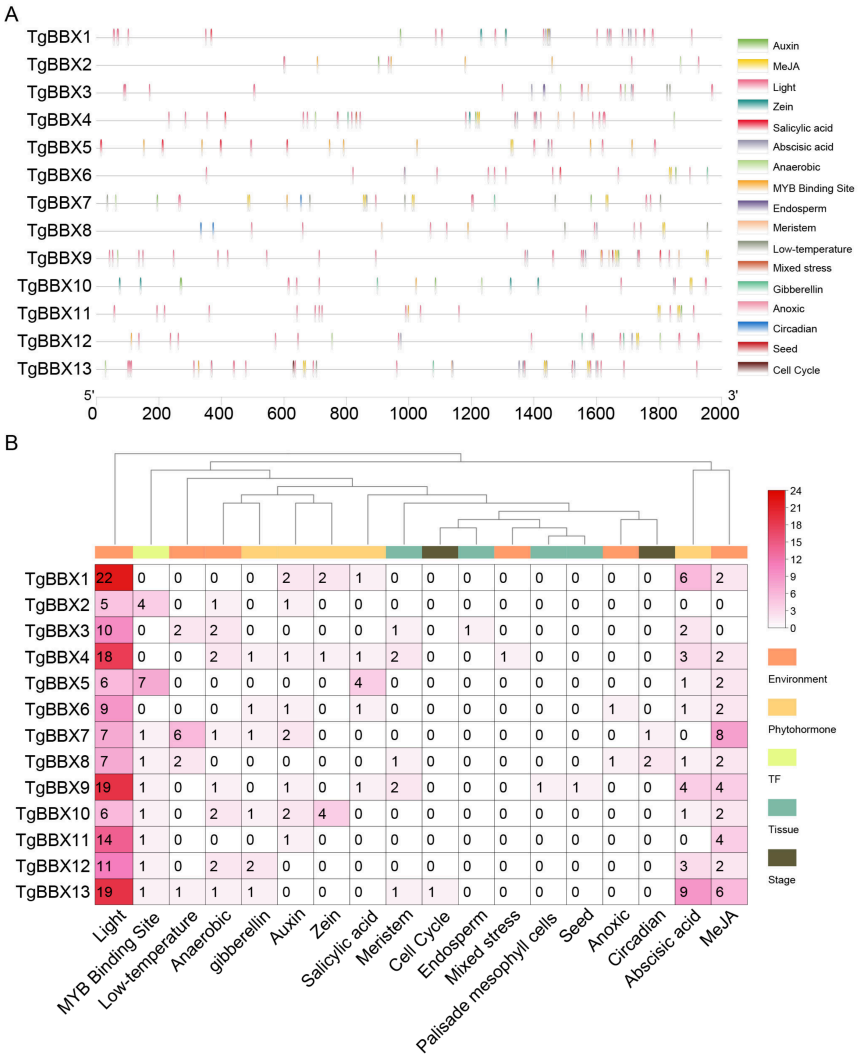


Figure 3. *Cis*-regulatory element analysis of *TgBBX* promoters. (**A**) Distribution of *cis*-elements in 2000 bp promoter sequences of *TgBBXs*. (**B**) Heatmap showing quantity of different *cis*-elements in each *TgBBX*.

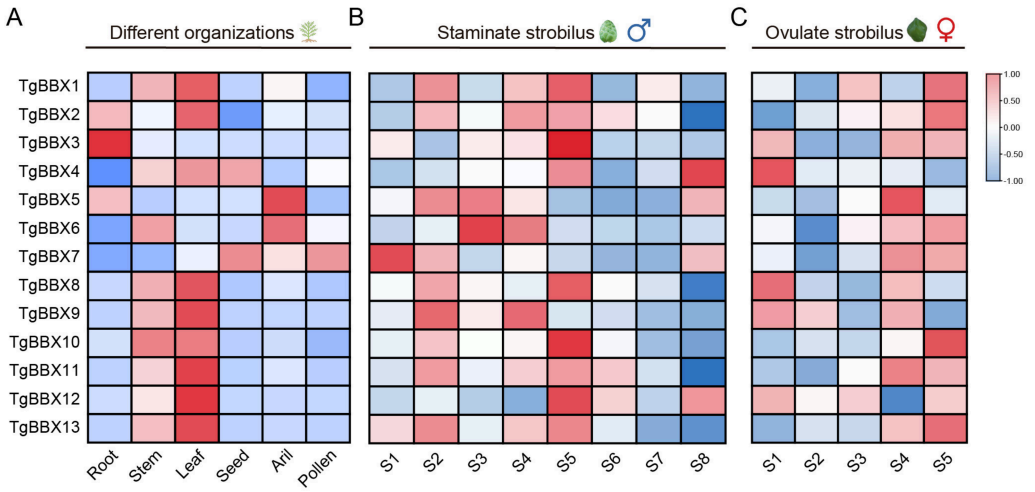


Figure 4. Tissue- and stage-specific expression profiles of *TgBBXs*. (**A**) Expression levels in six different vegetative and reproductive tissues (root, stem, leaf, seed, aril, pollen). (**B**) Expression patterns during eight developmental stages (S1–S8) of staminate strobili. (**C**) Expression patterns during five developmental stages (S1–S5) of ovulate strobili.

3.5. Phenotypic and Physiological Responses of T. grandis Seedlings to PEG-Simulated Drought Stress

To explore the roles of *TgBBXs* in abiotic stress responses of *T. grandis*, 30% PEG was used to simulate drought stress in hydroponically cultured *T. grandis* seedlings. Phenotypic and physiological changes were monitored at 0 h (CK), 2 h (S2), 8 h (S8), and 24 h (S24) after treatment. As shown in Figure 5A, leaf wilting and dehydration symptoms became progressively more severe with prolonged PEG exposure, with obvious leaf wilting observed at 24 h. Consistently with the phenotypic changes, chlorophyll a contents showed a significant decrease only at 24 h, while chlorophyll b and total chlorophyll contents were significantly reduced as early as 2 h after treatment, with a continuous decline over the stress period (Figure 5B–D). Further analysis of root physiological indicators revealed that hydrogen peroxide contents increased continuously with prolonged 30% PEG treatment (Figure 5E). Similarly, APX and POD activities rose notably starting from 2 h and peaked at 24 h (Figure 5F,G). These findings suggest that *T. grandis* seedlings activate antioxidant defense systems to alleviate oxidative damage under drought stress, and chlorophyll a degradation only takes place at the late stress stage.

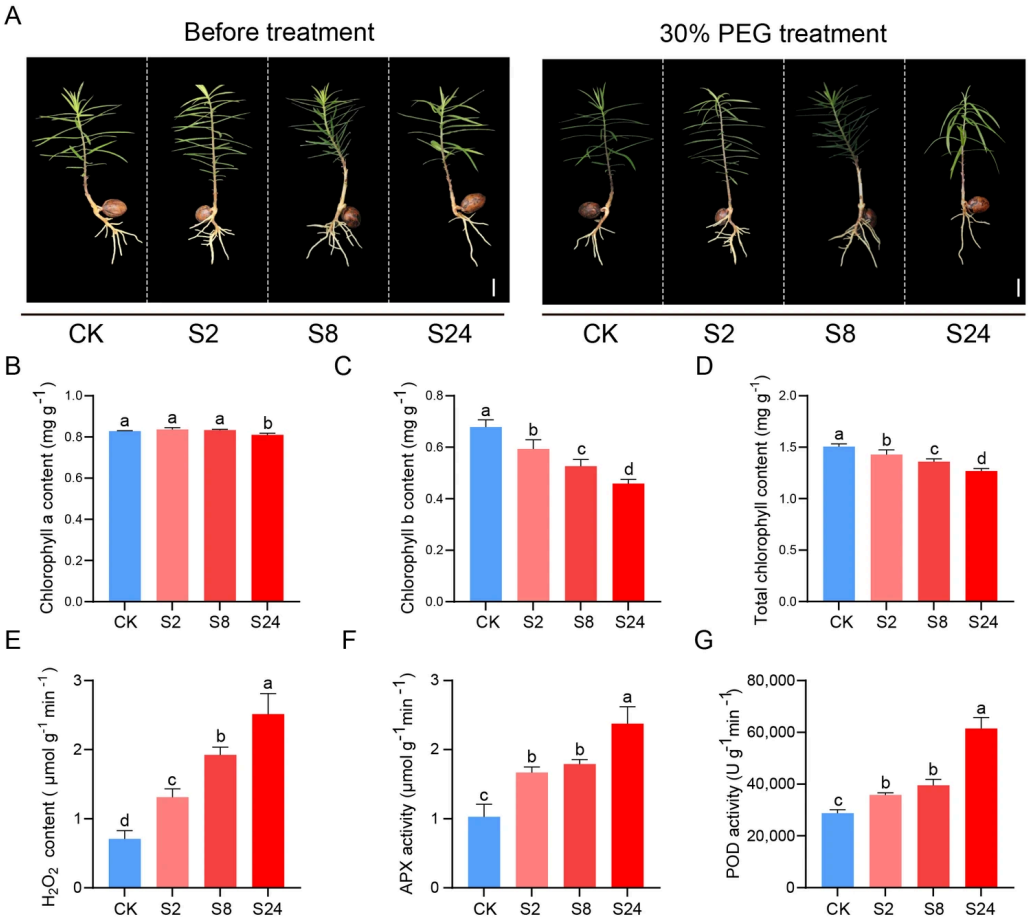


Figure 5. Morphological and physiological changes to *T. grandis* seedlings under PEG-simulated drought stress. (**A**) Seedling morphological features in CK (untreated control) and 2 h, 8 h and 24 h PEG treatment groups before and after drought treatment. Scale bar = 2.0 cm. (**B**–**D**) Quantification of chlorophyll a, chlorophyll b and total chlorophyll contents in seedling leaves under drought stress. (**E**) Quantification of H_2O_2 content in seedling roots under drought stress. (**F**,**G**) Quantification of APX and POD activities in seedling roots under drought stress. Error bars indicate standard deviation (SD, $n = 3$). Different letters indicate significant differences according to one-way ANOVA ($p < 0.05$).

3.6. Transcriptome Analysis Under PEG-Simulated Drought Stress

Transcriptome analysis was performed on leaves of *T. grandis* seedlings under 30% PEG-simulated drought stress, with samples collected at 0 h (CK_L), 2 h (S2_L), 8 h (S8_L), and 24 h (S24_L) post-treatment. High-quality transcriptome sequencing data were obtained for all samples (Table S2), and principal component analysis (PCA) revealed clear separation of transcriptome profiles across different treatment time points (Figure 6A). Differentially expressed gene analysis revealed varying numbers of upregulated and downregulated genes in each comparison (Table S3), with 1007 genes commonly regulated across all three treatments compared to the control (Figure 6B,C; Table S4). Further KEGG enrichment analysis of these core shared DEGs indicated that they were mainly enriched in pathways related to photosynthesis (ko00195), oxidative phosphorylation (ko00190), and protein processing in endoplasmic reticulum (ko04141), among others (Figure 6D, Table S5). Further analysis revealed that a large number of *TgBBXs*, including *TgBBX5* to *TgBBX12*, were significantly upregulated under PEG-simulated drought stress, with expression levels increasing continuously with the treatment duration (Figure 6E). In contrast, *TgBBX2*, *TgBBX3* and *TgBBX13* exhibited the opposite expression pattern.

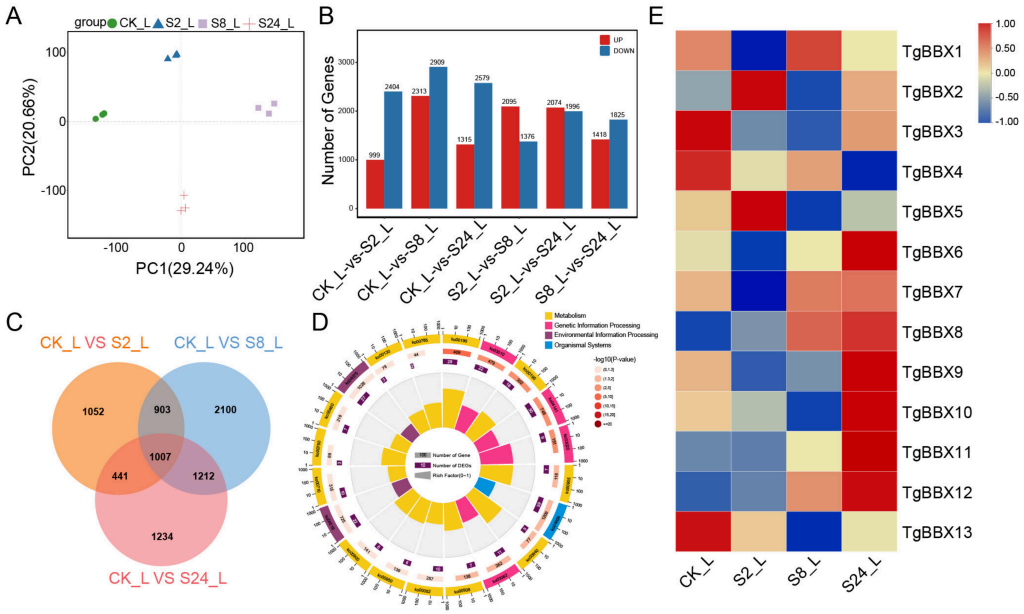


Figure 6. Transcriptome profiling of *T. grandis* leaves under PEG-simulated drought stress. (**A**) Principal component analysis. (**B**) Statistics of DEGs in each comparison group. (**C**) Venn diagram displaying shared DEGs among different drought treatments. (**D**) KEGG pathway enrichment analysis of shared DEGs. (**E**) Expression heatmap of 13 *TgBBXs* under different drought treatments. Gene expression values were normalized using Z-score transformation for comparative visualization.

To further explore the drought response mechanism in underground tissues, transcriptome profiling was subsequently conducted on root tissues of *T. grandis* seedlings under the same PEG treatment condition. PCA showed clear separation of transcriptome profiles across the 0 h (CK_R), 2 h (S2_R), 8 h (S8_R) and 24 h (S24_R) treatment groups (Figure 7A), with 1856 core shared DEGs identified among all three stress comparisons (Figure 7B,C; Tables S6 and S7). These shared drought-responsive genes were enriched in key pathways including plant hormone signal transduction (ko04075), galactose metabolism (ko00052), and plant–pathogen interaction (ko04626) (Figure 7D, Table S8). Unlike the expression patterns observed in leaves, most root *TgBBXs*, including *TgBBX1–3* and *TgBBX10–12*, were significantly downregulated under PEG-simulated drought stress. In contrast, *TgBBX5* and *TgBBX7* were markedly upregulated specifically at 24 h of PEG treatment (Figure 7E).

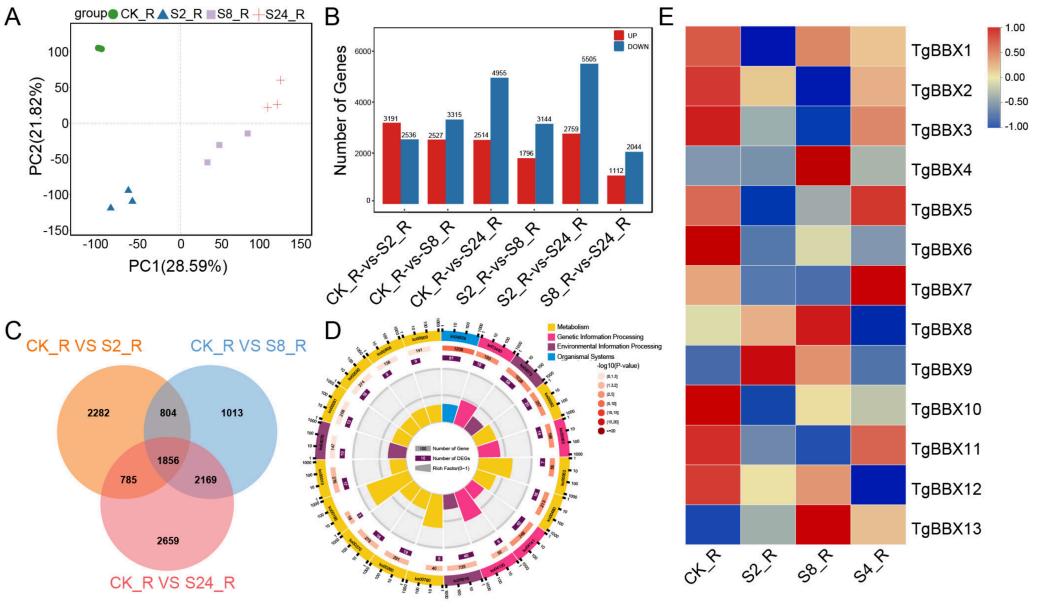


Figure 7. Transcriptome profiling of *T. grandis* roots under PEG-simulated drought stress. (**A**) Principal component analysis. (**B**) Statistics of DEGs in each comparison group. (**C**) Venn diagram displaying shared DEGs among different drought treatments. (**D**) KEGG pathway enrichment analysis of shared DEGs. (**E**) Expression heatmap of 13 *TgBBXs* under different drought treatments. Gene expression values were normalized using Z-score transformation for comparative visualization.

3.7. Construction of the Potential Regulatory Network of TgBBXs

To further identify key *TgBBXs* under PEG-simulated drought stress, WGCNA was performed via the R WGCNA package using FPKM values from 24 samples and six physiological traits. Normalization and filtering were conducted following the default built-in procedures of the R WGCNA package, and 28,455 genes were retained to construct the co-expression network. The adjacency matrix was set at a soft-thresholding value of β = 14, and the average gene connectivity was 711 (Figure 8A). After hierarchical clustering via WGCNA, these genes were grouped into 11 modules (Figure 8B, Table S9), and Pearson correlation analysis was performed to evaluate their internal relationships (Figure S1). Further module–trait correlation analysis based on the correlation coefficients and significance levels ($p < 0.05$) of each module with physiological traits indicated that chlorophyll b and total chlorophyll were positively associated with MEturquoise but significantly negatively associated with MEblack (Figure 8C). POD, APX and H_2O_2 contents were significantly positively correlated with MEbrown and negatively correlated with MEturquoise (Figure 8C), implying MEturquoise as the core module. Nevertheless, the 13 *TgBBXs* were distributed across distinct modules: most members, including *TgBBX2* and *TgBBX5*–*TgBBX13*, were clustered in MEturquoise, while *TgBBX3* and *TgBBX4* belonged to MEblue, and *TgBBX1* was assigned to MEblack (Table S10). Notably, *TgBBX2*, *TgBBX7* and *TgBBX13* exhibited a gene module membership value greater than 0.9, implying that these three genes may function as hub candidates within the corresponding module. Further KEGG enrichment analysis revealed that genes in MEturquoise were mainly enriched in photosynthesis- and chlorophyll-related pathways, such as photosynthesis—antenna proteins, porphyrin metabolism, and biosynthesis of cofactors, as well as oxidative stress-related pathways including ribosome, RNA degradation and selenocompound metabolism (Figure 8D and Table S11). These results indicate that *TgBBX2*, *TgBBX7* and *TgBBX13* are potential candidate genes linked to photosynthetic regulation and oxidative stress tolerance under PEG-simulated drought stress and may participate in the drought response

process of *T. grandis*. Further functional verification is still required to confirm their direct regulatory roles.

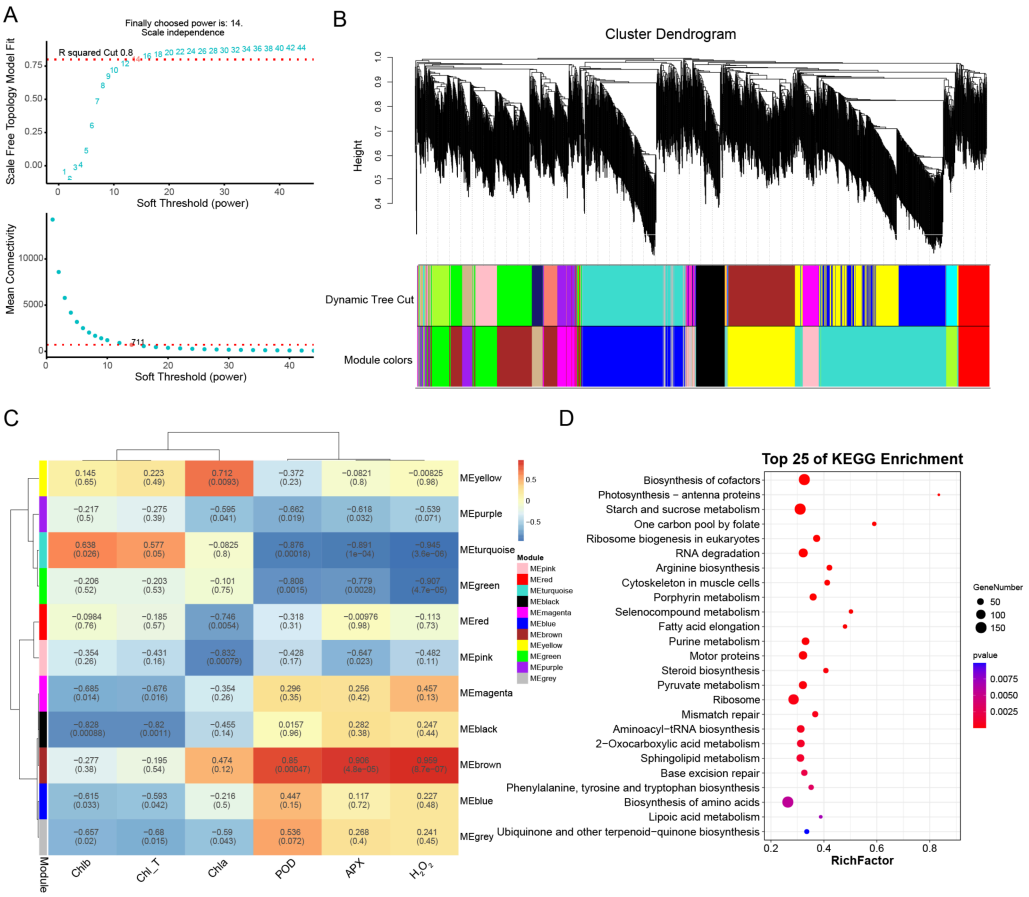


Figure 8. WGCNA based on transcriptomic and physiological data under PEG-simulated drought stress. (**A**) Filtering appropriate soft thresholds. (**B**) Hierarchical clustering tree of all expressed genes and corresponding module. (**C**) Heatmap displaying correlations between eigengene modules and six physiological indices. (**D**) Top 25 enriched KEGG pathways of genes within MEturquoise module.

4. Discussion

BBX transcription factors are key regulators of plant growth, development, and stress responses [1,10]. Their functions have been extensively studied in angiosperms such as Arabidopsis, rice, and tomato [5,6,30]. However, as a major branch of the plant kingdom, gymnosperms remain largely unexplored regarding the evolutionary characteristics and stress-resistant functions of their BBX gene families.

In this study, we identified 13 *TgBBXs* at the genome-wide level for the first time in *T. grandis*, an ancient relict gymnosperm and a highly nutritious nut crop widely cultivated in China [21,31]. This number of *TgBBXs* is similar to that in other gymnosperms, such as *G. biloba* (14), *W. mirabilis* (13), and *C. panzhihuaensis* (11), but considerably smaller than that in angiosperms, including *A. thaliana* (32), *G. max* (59), and *Z. mays* (36) [5,6,8,9]. Consistently with previous comparative genomics reports on seed plants, our observation supports that gymnosperm BBX families retain a relatively stable gene number and have not undergone frequent whole-genome duplication and tandem duplication events that drive large-scale BBX expansion in flowering plants [10,32]. Phylogenetic analysis further revealed distinct evolutionary divergence among BBXs from *A. thaliana*, *T. grandis*, and other representative gymnosperms. AtBBXs were widely distributed across all five clades and exhibited obvious family expansion, while gymnosperm BBXs were relatively concentrated and displayed a more conservative evolutionary profile. Notably, clade 3 was predomi-

nantly occupied by gymnosperm sequences, suggesting that this clade may represent a gymnosperm-specific evolutionary branch. In contrast, almost no TgBBXs were assigned to this clade, which may imply a unique evolutionary pattern and potential functional differentiation of the BBX family in Taxaceae within gymnosperms.

In terms of protein structure, TgBBXs can be classified into four categories: the double B-box type (TgBBX1-5), double B-box+CCT type (TgBBX6-9), single B-box+CCT type (TgBBX11-13), and single B-box type (TgBBX10). This classification is highly consistent with that for *A. thaliana*, indicating that the core structure of the BBX family was basically formed before the divergence of seed plants [5]. Promoter *cis*-acting element analysis revealed that the promoter regions of all *TgBBXs* are highly enriched in light-responsive elements and also contain abundant hormone-responsive and stress-responsive elements. Functional studies in Arabidopsis have verified that AtBBX30 and AtBBX31 act as negative regulators of photomorphogenesis, wherein the central light signaling regulator AtHY5 directly targets the G-box motifs in their promoters and suppresses their light-dependent transcription [33]. Similarly, the light-induced BBX member LvBBX24 in horticultural plants synergistically interacts with LvbZIP44 to activate anthocyanin biosynthesis in lily petals [34]. Combined with our structural and *cis*-element analysis of *TgBBXs*, these conserved features across seed plant BBX homologs suggest that multisignal integration may be an ancestral function of BBX families [1,35]. Our findings expand related theories by confirming that gymnosperm *TgBBXs* also possess the genetic basis to respond to light hormone and stress signals through abundant promoter cis-elements. Tissue expression analysis revealed distinct tissue-specific expression patterns of *TgBBXs* in *T. grandis*. Most members were highly expressed in leaves and stems, consistently with the functions of *AtBBXs* and *OsBBXs* in mediating light signaling and photosynthetic regulation [1]. Notably, *TgBBXs* display sex-divergent expression patterns between staminate and ovulate strobili. This sex-biased expression pattern resembles the regulatory mode of *TkBBXs* in the dioecious herb *Trichosanthes kirilowii*, where several TkBBX homologs show opposite expression trends in male and female flowers [36]. These findings suggest that *BBX* exerts conserved functions in regulating reproductive development and sex differentiation in seed plants. Our observation of differential BBX expression between staminate and ovulate strobili of *T. grandis* supplements gymnosperm reproductive regulatory research.

To elucidate the drought adaptation mechanism of *T. grandis*, we treated seedlings with 30% PEG to mimic drought and investigated their physiological changes. Drought stress caused a notable decline in chlorophyll b contents, along with elevated H_2O_2 contents and increased activities of APX and POD in roots. Similar physiological adjustments have been widely documented in conifer and Taxus species under PEG-simulated drought, whereby roots frequently activate antioxidant responses in the early phase of stress to scavenge ROS and preserve root capacity for water uptake [37,38]. This suggests that *T. grandis* enhances root ROS scavenging capacity to sustain redox balance and mitigate oxidative injury. Further, WGCNA showed that the core MEturquoise module contains genes related to photosynthetic antenna proteins, porphyrin metabolism and cofactor biosynthesis. Most *TgBBXs*, especially *TgBBX2*, *TgBBX7* and *TgBBX13*, were core members of the MEturquoise module. Functional enrichment analysis indicated that genes in this module primarily participate in photosynthetic metabolism and oxidative stress regulation. In Arabidopsis, BBX21 promotes photomorphogenesis by activating *HY5* and serves as a key component in photosynthetic regulation [39]. Additionally, BBX14 contributes to chlorophyll biosynthesis and chloroplast development by linking the GUN1–GLK1 retrograde signaling pathway to photosynthetic competence [40]. In tomato, BBX family members such as SlBBX20 and SlBBX21 participate in light signal transduction and photosynthetic pathways, thereby regulating photomorphogenesis and photosynthetic efficiency [41–43]. Notably, BBX proteins

also exhibit diverse regulatory functions in drought-induced oxidative stress. For instance, SlBBX18 negatively regulates drought tolerance by directly repressing *APX1* transcription in tomato [17]. In sweet potato, the IbBBX24–IbTOE3–IbPRX17 module strengthens abiotic stress tolerance through clearing reactive oxygen species [44]. Similarly, silencing of AhBBX6 demonstrates that this transcription factor positively regulates the activities of SOD, POD and CAT; reduces H_2O_2 accumulation; and enhances drought and salt tolerance in peanut [45].

Collectively, our findings demonstrate that the BBX gene family in *T. grandis* is evolutionarily conserved yet structurally and functionally distinct from counterparts in angiosperms. Our integrated physiological and co-expression analysis only detected significant correlative associations between the hub genes *TgBBX2*, *TgBBX7* and *TgBBX13* and photosynthetic metabolism, as well as antioxidant pathways under drought stress. Based on the present co-expression dataset, we put forward a testable hypothesis that these three *TgBBXs* may be associated with chlorophyll maintenance and ROS scavenging processes controlled by APX and POD. These correlative observations lead us to speculate that *TgBBXs* could serve as candidate molecular connectors linking light signaling, photosynthetic homeostasis and drought-induced oxidative stress tolerance, which might contribute to the strong drought adaptability of *T. grandis*. Nevertheless, our physiological assessment of drought response has certain drawbacks. We only measured chlorophyll- and antioxidant-related physiological indicators to evaluate drought-induced oxidative stress response, while critical parameters directly reflecting plant water status, including relative water content, electrolyte leakage and water potential, were not detected due to the limited experimental period and sampling conditions. Supplementary measurement of these water-related physiological indices can more comprehensively reveal the water loss status and cell membrane damage degree of *T. grandis* under drought stress in future research.

5. Conclusions

In conclusion, this study presents the first genome-wide identification and systematic analysis of the *BBX* family in *T. grandis*. Thirteen *TgBBXs* were identified and classified into four structural groups, displaying evolutionary conservation and gymnosperm-specific characteristics. Promoter *cis*-element analysis indicated extensive involvement of TgBBXs in light response, hormone signaling and stress adaptation. Expression profiling revealed tissue-specific patterns and strong drought responsiveness in both leaves and roots. Physiological measurements showed that drought stress triggers chlorophyll reduction, ROS accumulation and activation of antioxidant enzymes including APX and POD. WGCNA further identified *TgBBX2*, *TgBBX7* and *TgBBX13* as core members of the MEturquoise module, whose eigengene exhibits significant correlative relationships with chlorophyll content and antioxidant enzyme activities under drought treatment. Genes in this module were mainly enriched in photosynthetic metabolism and oxidative stress regulation. Together, these correlative findings raise a testable hypothesis that *TgBBXs* are linked to the coordination of photosynthetic maintenance and antioxidant defense under drought stress. This work provides valuable candidate genes and a preliminary theoretical reference for subsequent molecular functional verification of drought tolerance in *T. grandis*.

Supplementary Materials: The following supporting information can be downloaded at https://www.mdpi.com/article/10.3390/horticulturae12080932/s1.

Author Contributions: W.C.: Methodology, Validation, Investigation, Writing—original draft. X.Z.: Methodology, Validation, Investigation. F.D.: Validation. X.L.: Validation. C.Z.: Writing—review and

editing, Validation, Resources. J.W.: Writing—review and editing, Supervision. All authors have read and agreed to the published version of the manuscript.

Funding: This research was supported by the National Natural Science Foundation of China (32572099), Zhejiang Provincial Natural Science Foundation of China (LQN25C160005), Zhejiang Provincial Natural Science Foundation of China (LQK26C160001), and Scientific Research Startup Fund Project of Zhejiang A&F University (2024LFR119).

Data Availability Statement: The original contributions presented in this study are included in the article. Further inquiries can be directed to the corresponding authors.

Conflicts of Interest: The authors declare no conflicts of interest.

References

1. Gangappa, S.N.; Botto, J.F. The BBX family of plant transcription factors. *Trends Plant Sci.* **2014**, *19*, 460–470. [CrossRef] [PubMed]
2. Meroni, G.; Diez-Roux, G. TRIM/RBCC, a novel class of 'single protein RING finger' E3 ubiquitin ligases. *BioEssays* **2005**, *27*, 1147–1157. [CrossRef] [PubMed]
3. Son, S.H.; Lee, M.K.; Son, Y.E.; Park, H.S. HbxB is a key regulator for stress response and β-glucan biogenesis in *Aspergillus nidulans*. *Microorganisms* **2021**, *9*, 144. [CrossRef] [PubMed]
4. Crocco, C.D.; Botto, J.F. BBX proteins in green plants: Insights into their evolution, structure, feature and functional diversification. *Gene* **2013**, *531*, 44–52. [CrossRef] [PubMed]
5. Khanna, R.; Kronmiller, B.; Maszle, D.R.; Coupland, G.; Holm, M.; Mizuno, T.; Wu, S.H. The Arabidopsis B-box zinc finger family. *Plant Cell* **2009**, *21*, 3416–3420. [CrossRef] [PubMed]
6. Shan, B.; Bao, G.; Shi, T.; Zhai, L.; Bian, S.; Li, X. Genome-wide identification of BBX gene family and their expression patterns under salt stress in soybean. *BMC Genom.* **2022**, *23*, 820. [CrossRef]
7. Xue, Y.; Chen, J.; Hao, J.; Bao, X.; Kuang, L.; Zhang, D.; Zong, C. Identification of the BBX gene family in blueberry at different chromosome ploidy levels and fruit development and response under stress. *BMC Genom.* **2025**, *26*, 100. [CrossRef]
8. Xu, X.H.; Li, W.L.; Yang, S.K.; Zhu, X.Z.; Sun, H.W.; Li, F.; Lu, X.B.; Cui, J.J. Identification, evolution, expression and protein interaction analysis of genes encoding B-box zinc-finger proteins in maize. *J. Integr. Agric.* **2023**, *22*, 371–388. [CrossRef]
9. Huang, J.; Zhao, X.; Weng, X.; Wang, L.; Xie, W. The rice B-box zinc finger gene family: Genomic identification, characterization, expression profiling and diurnal analysis. *PLoS ONE* **2012**, *7*, e48242. [CrossRef] [PubMed]
10. Jiang, Y.; Lei, P.; Ji, X.; Li, J.; Zhao, Y.; Jiang, M.; Ma, L.; Zhao, X.; Meng, F. B-BOX PROTEINS (BBXs) transcription factors in plant: A comprehensive review of their growth, development, abiotic stress responses and phytohormone signals. *Plant Stress* **2025**, *18*, 101042. [CrossRef]
11. Putterill, J.; Robson, F.; Lee, K.; Simon, R.; Coupland, G. The CONSTANS gene of arabidopsis promotes flowering and encodes a protein showing similarities to zinc finger transcription factors. *Cell* **1995**, *80*, 847–857. [CrossRef] [PubMed]
12. Suárez-López, P.; Wheatley, K.; Robson, F.; Onouchi, H.; Valverde, F.; Coupland, G. CONSTANS mediates between the circadian clock and the control of flowering in Arabidopsis. *Nature* **2001**, *410*, 1116–1120. [CrossRef] [PubMed]
13. Wang, H.; Pan, J.; Li, Y.; Lou, D.; Hu, Y.; Yu, D. The DELLA-CONSTANS Transcription Factor Cascade Integrates Gibberellic Acid and Photoperiod Signaling to Regulate Flowering. *Plant Physiol.* **2016**, *172*, 479–488. [CrossRef] [PubMed]
14. Böhlenius, H.; Huang, T.; Charbonnel-Campaa, L.; Brunner, A.M.; Jansson, S.; Strauss, S.H.; Nilsson, O. CO/FT Regulatory Module Controls Timing of Flowering and Seasonal Growth Cessation in Trees. *Science* **2006**, *312*, 1040–1043. [CrossRef] [PubMed]
15. Jiang, L.; Wang, Y.; Li, Q.F.; Björn, L.O.; He, J.X.; Li, S.S. Arabidopsis STO/BBX24 negatively regulates UV-B signaling by interacting with COP1 and repressing HY5 transcriptional activity. *Cell Res.* **2012**, *22*, 1046–1057. [CrossRef] [PubMed]
16. Luo, D.; Xiong, C.; Lin, A.; Zhang, C.; Sun, W.; Zhang, J.; Yang, C.; Lu, Y.; Li, H.; Ye, Z.; et al. SlBBX20 interacts with the COP9 signalosome subunit SlCSN5-2 to regulate anthocyanin biosynthesis by activating *SlDFR* expression in tomato. *Hortic. Res.* **2021**, *8*, 163. [CrossRef] [PubMed]
17. Li, J.; Ai, G.; Wang, Y.; Ding, Y.; Hu, X.; Liang, Y.; Yan, Q.; Wu, K.; Huang, R.; Chen, C.; et al. A truncated B-box zinc finger transcription factor confers drought sensitivity in modern cultivated tomatoes. *Nat. Commun.* **2024**, *15*, 8013. [CrossRef] [PubMed]
18. Dong, J.; Zhao, C.; Zhang, J.; Ren, Y.; He, L.; Tang, R.; Wang, W.; Jia, X. The sweet potato B-box transcription factor gene IbBBX28 negatively regulates drought tolerance in transgenic Arabidopsis. *Front. Genet.* **2022**, *13*, 1077958. [CrossRef] [PubMed]
19. Zhou, W.; Harris, A.J.; Xiang, Q.Y. Phylogenomics and biogeography of *Torreya* (Taxaceae)—Integrating data from three organelle genomes, morphology, and fossils and a practical method for reducing missing data from RAD-seq. *J. Syst. Evol.* **2022**, *60*, 1241–1262. [CrossRef]
20. Suo, J.; Liu, Y.; Yan, J.; Li, Q.; Chen, W.; Liu, Z.; Zhang, Z.; Hu, Y.; Yu, W.; Yan, J.; et al. Sucrose promotes cone enlargement via the TgNGA1-TgWRKY47-TgEXPA2 module in *Torreya grandis*. *New Phytol.* **2024**, *243*, 1823–1839. [CrossRef] [PubMed]

21. Suo, J.; Ma, Z.; Zhao, B.; Ma, S.; Zhang, Z.; Hu, Y.; Yang, B.; Yu, W.; Wu, J.; Song, L. Metabolomics reveal changes in flavor quality and bioactive components in post-ripening *Torreya grandis* nuts and the underlying mechanism. *Food Chem.* **2023**, *406*, 134987. [CrossRef] [PubMed]
22. Lou, H.; Song, L.; Li, X.; Zi, H.; Chen, W.; Gao, Y.; Zheng, S.; Fei, Z.; Sun, X.; Wu, J. The *Torreya grandis* genome illuminates the origin and evolution of gymnosperm-specific sciadonic acid biosynthesis. *Nat. Commun.* **2023**, *14*, 1315. [CrossRef] [PubMed]
23. Marchler-Bauer, A.; Derbyshire, M.K.; Gonzales, N.R.; Lu, S.; Chitsaz, F.; Geer, L.Y.; Geer, R.C.; He, J.; Gwadz, M.; Hurwitz, D.I.; et al. CDD: NCBI's conserved domain database. *Nucleic Acids Res.* **2015**, *43*, D222–D226. [PubMed]
24. Rozewicki, J.; Li, S.; Amada, K.M.; Standley, D.M.; Katoh, K. MAFFT-DASH: Integrated protein sequence and structural alignment. *Nucleic Acids Res.* **2019**, *47*, W5–W10. [CrossRef] [PubMed]
25. Nguyen, L.T.; Schmidt, H.A.; von Haeseler, A.; Minh, B.Q. IQ-TREE: A Fast and Effective Stochastic Algorithm for Estimating Maximum-Likelihood Phylogenies. *Mol. Biol. Evol.* **2014**, *32*, 268–274. [CrossRef] [PubMed]
26. He, Z.; Zhang, H.; Gao, S.; Lercher, M.J.; Chen, W.H.; Hu, S. Evolview v2: An online visualization and management tool for customized and annotated phylogenetic trees. *Nucleic Acids Res.* **2016**, *44*, W236–W241. [CrossRef] [PubMed]
27. Lescot, M.; Déhais, P.; Thijs, G.; Marchal, K.; Moreau, Y.; Van de Peer, Y.; Rouzé, P.; Rombauts, S. PlantCARE, a database of plant cis-acting regulatory elements and a portal to tools for in silico analysis of promoter sequences. *Nucleic Acids Res.* **2002**, *30*, 325–327. [CrossRef] [PubMed]
28. Chen, C.; Wu, Y.; Li, J.; Wang, X.; Zeng, Z.; Xu, J.; Liu, Y.; Feng, J.; Chen, H.; He, Y.; et al. TBtools-II: A "one for all, all for one" bioinformatics platform for biological big-data mining. *Mol. Plant.* **2023**, *16*, 1733–1742. [CrossRef] [PubMed]
29. Kim, D.; Paggi, J.M.; Park, C.; Bennett, C.; Salzberg, S.L. Graph-based genome alignment and genotyping with HISAT2 and HISAT-genotype. *Nat. Biotechnol.* **2019**, *37*, 907–915. [CrossRef] [PubMed]
30. Song, J.; Lin, R.; Tang, M.; Wang, L.; Fan, P.; Xia, X.; Yu, J.; Zhou, Y. SlMPK1- and SlMPK2-mediated SlBBX17 phosphorylation positively regulates CBF-dependent cold tolerance in tomato. *New Phytol.* **2023**, *239*, 1887–1902. [CrossRef] [PubMed]
31. Yan, J.; Zeng, H.; Chen, W.; Zheng, S.; Luo, J.; Jiang, H.; Yang, B.; Farag, M.A.; Lou, H.; Song, L.; et al. Effects of tree age on flavonoids and antioxidant activity in *Torreya grandis* nuts via integrated metabolome and transcriptome analyses. *Food Front.* **2023**, *4*, 358–367. [CrossRef]
32. Yu, L.; Lyu, Z.; Liu, H.; Zhang, G.; He, C.; Zhang, J. Insights into the evolutionary origin and expansion of the BBX gene family. *Plant Biotechnol. Rep.* **2022**, *16*, 205–214. [CrossRef]
33. Heng, Y.; Lin, F.; Jiang, Y.; Ding, M.; Yan, T.; Lan, H.; Zhou, H.; Zhao, X.; Xu, D.; Deng, X.W. B-Box containing proteins BBX30 and BBX31, acting downstream of HY5, negatively regulate photomorphogenesis in *Arabidopsis*. *Plant Physiol.* **2019**, *180*, 497–508. [CrossRef]
34. Gao, Z.; Sun, Y.; Zhu, Z.; Ni, N.; Sun, S.; Nie, M.; Du, W.; Irfan, M.; Chen, L.; Zhang, L. Transcription factors LvBBX24 and LvbZIP44 coordinated anthocyanin accumulation in response to light in lily petals. *Hortic. Res.* **2024**, *11*, uhae211. [CrossRef] [PubMed]
35. Cao, J.; Yuan, J.; Zhang, Y.; Chen, C.; Zhang, B.; Shi, X.; Niu, R.; Lin, F. Multi-layered roles of BBX proteins in plant growth and development. *Stress Biol.* **2023**, *3*, 1. [CrossRef] [PubMed]
36. Li, W.; Xiong, R.; Chu, Z.; Peng, X.; Cui, G.; Dong, L. Transcript-wide identification and characterization of the BBX gene family in *Trichosanthes kirilowii* and its potential roles in development and abiotic stress. *Plants* **2025**, *14*, 975. [CrossRef] [PubMed]
37. Xu, D.; Jiang, Y.; Li, J.; Lin, F.; Holm, M.; Deng, X.W. BBX21, an Arabidopsis B-box protein, directly activates HY5 and is targeted by COP1 for 26S proteasome-mediated degradation. *Proc. Natl. Acad. Sci. USA* **2016**, *113*, 7655–7660. [CrossRef] [PubMed]
38. Sarmadi, M.; Karimi, N.; Palazón, J.; Ghassempour, A.; Mirjalili, M.H. Physiological, biochemical, and metabolic responses of a *Taxus baccata* L. callus culture under drought stress. *Vitr. Cell. Dev. Biol.-Plant* **2020**, *56*, 703–717. [CrossRef]
39. Xiao, F.; Zhao, Y.; Wang, X.; Jian, X.; Yang, Y. Physiological responses to drought stress of three pine species and comparative transcriptome analysis of *Pinus yunnanensis* var. *pygmaea*. *BMC Genom.* **2024**, *25*, 281. [CrossRef]
40. Atanasov, V.; Schumacher, J.; Muiño, J.M.; Larasati, C.; Wang, L.; Kaufmann, K.; Leister, D.; Kleine, T. Arabidopsis BBX14 is involved in high light acclimation and seedling development. *Plant J.* **2024**, *118*, 141–158. [PubMed]
41. Bu, X.; Wang, X.; Yan, J.; Zhang, Y.; Zhou, S.; Sun, X.; Yang, Y.; Ahammed, G.J.; Liu, Y.; Qi, M.; et al. Genome-wide characterization of B-box gene family and its roles in responses to light quality and cold stress in Tomato. *Front. Plant Sci.* **2021**, *12*, 698525. [CrossRef] [PubMed]
42. Ma, Y.; Xu, Z.; Wang, L.; Ding, R.; Zhang, Y.; Wang, J.; Wang, P.; Yao, W.; Li, X.; Li, G.; et al. The light-responsive transcription factor SlBBX20 improves saline-alkali resistance of *Solanum lycopersicum* by affecting photosynthetic capacity, antioxidant capacity, and osmotic adjustment. *Environ. Exp. Bot.* **2024**, *224*, 105818. [CrossRef]
43. Yang, G.; Zhang, C.; Dong, H.; Liu, X.; Guo, H.; Tong, B.; Fang, F.; Zhao, Y.; Yu, Y.; Liu, Y.; et al. Activation and negative feedback regulation of SlHY5 transcription by the SlBBX20/21–SlHY5 transcription factor module in UV-B signaling. *Plant Cell* **2022**, *34*, 2038–2055. [CrossRef] [PubMed]

44. Zhang, H.; Wang, Z.; Li, X.; Gao, X.; Dai, Z.; Cui, Y.; Zhi, Y.; Liu, Q.; Zhai, H.; Gao, S.; et al. The IbBBX24–IbTOE3–IbPRX17 module enhances abiotic stress tolerance by scavenging reactive oxygen species in sweet potato. *New Phytol.* **2022**, *233*, 1133–1152. [PubMed]
45. Tang, H.; Yuan, C.; Shi, H.; Liu, F.; Shan, S.; Wang, Z.; Sun, Q.; Sun, J. Genome-wide identification of peanut B-boxs and functional characterization of AhBBX6 in salt and drought stresses. *Plants* **2024**, *13*, 955. [CrossRef] [PubMed]

Disclaimer/Publisher's Note: The statements, opinions and data contained in all publications are solely those of the individual author(s) and contributor(s) and not of MDPI and/or the editor(s). MDPI and/or the editor(s) disclaim responsibility for any injury to people or property resulting from any ideas, methods, instructions or products referred to in the content.